International Journal of Fatigue 180 (2024) 108108

Contents lists available at ScienceDirect

International Journal of Fatigue

journal homepage: www.elsevier.com/locate/ijfatigue

Experimental Data-Driven approach for the evaluation of crack tip opening loads under variable amplitude loading

Andrei Kotousov [a,*], James Hughes [a], Aditya Khanna [b], Belen Moreno [c], Chris Wallbrink [d]

[a] School of Mechanical Engineering, The University of Adelaide, SA 5005, Australia
[b] School of Mechanical & Mining Engineering, The University of Queensland, QLD 4072, Australia
[c] Department of Civil and Materials Engineering, University of Malaga, Spain
[d] Platforms, Defence Science and Technology Group, VIC 3207, Australia

ARTICLE INFO

Keywords:
Data-driven approach
Crack closure
Variable amplitude loading
Crack tip opening load
Effective stress intensity factor range, CT specimen

ABSTRACT

In this paper, we present a new data-driven approach for the evaluation of crack tip opening load (P_{op}) values under variable amplitude loading. These values are analysed for CT specimens manufactured from common aircraft grade aluminium alloys and subjected to several load sequences, all of which have a relatively high R-ratio content without significant overloads and underloads. Direct experimental measurements and outcomes of numerical simulations indicate that the P_{op} change abruptly from cycle to cycle. For this type of fatigue loading (including a military transport aircraft load spectrum with more than 400,000 turning points) and materials, it was found that P_{op} is well described by a linear function of the preceding minimum and maximum values of the applied loading. This finding provides a new simple way to evaluate the effective stress intensity factor range, which is often considered as a fatigue crack driving force. It is also verified via the use of machine learning that the proposed approach is capable of predicting the mean stress (R-ratio) effect on P_{op} for block loading. Therefore, the developed data-driven approach is a promising alternative to the computational methods, which currently dominate advanced fatigue life assessment procedures.

1. Introduction

Loading cycles of variable amplitude are typical in aerospace, marine, wind turbine, transport, pipeline and many other applications [1]. Despite decades of extensive research, the evaluation of fatigue life of structural components working under Variable Amplitude Loading (VAL) remains very challenging [1–4]. This is the broad consensus amongst the international fracture community. One of the main challenges is the large variability in fatigue life predictions due to a number of problems and deficiencies in the current fatigue life assessment procedures, which will be discussed later in this paper. If the variability is not accounted for correctly, it could adversely affect safety, or alternatively, could lead to uneconomic usage and unnecessary or premature retirement of structures and load-bearing components.

At the core of many advanced fatigue life assessment procedures (numerical or analytical) is the crack tip opening/closure model, which aims to simulate the crack closure phenomenon [5–7]. Crack closure implies that a fatigue crack remains closed for some portion of a tensile load cycle due to the formation of a plastic wake behind the crack tip. This phenomenon was first discovered by Wolf Elber in 1970 during his PhD candidature at the University of New South Wales, Australia [8]. Since this discovery, there has been an exponential growth of research efforts directed to investigate crack closure mechanisms; the latter play an important role in understanding and modelling of fatigue crack propagation phenomena. In particular, the plasticity-induced crack closure leads to a reduction of the fatigue crack driving force, which is often considered to be a function of the effective stress intensity factor range, ΔK_{eff}. Other less common measures of fatigue crack driving force utilised in life assessments include non-linear parameters such as crack tip opening displacement (CTOD), plastic CTOD and cumulative plastic strain [9,10].

Crack tip opening loads and ΔK_{eff} can be evaluated using theoretical approaches including the Finite Element (FE) method. However, the application of the three-dimensional (3D) FE method for a large number of fatigue cycles is not feasible due to high computational power demands and extremely complex nature of the problem. Its application requires implementation of a crack advance scheme, re-meshing procedure and 3D modelling of contact between the crack surfaces in the

* Corresponding author.
E-mail address: andrei.kotousov@adelaide.edu.au (A. Kotousov).

https://doi.org/10.1016/j.ijfatigue.2023.108108
Received 21 August 2023; Received in revised form 15 November 2023; Accepted 12 December 2023
Available online 18 December 2023

presence of large plastic deformations. The methodology of such simulations is not well established and numerical results have only been reported for a limited number of fatigue cycles or particular loading sequences [11–18]. Pommier [19] has recently presented a methodology to overcome the shortcomings of direct FE simulations by employing a multiscale approach that combines elastic and elastic–plastic analysis to accelerate computation. However, this methodology needs further validation.

Simplified theoretical and computational models of Plasticity-Induced Crack Closure (PICC) rely on many assumptions, and among the most common is the 2D strip-yield idealisation suggested by Dugdale in 1960 [20]. This model allows for computationally efficient simulation of the plasticity effects associated with crack propagation, thereby making the underlying framework feasible for use in the fatigue life assessment procedures [1,3,4,21–23]. However, such assumptions may inevitably lead to large discrepancies between theoretical predictions and experimental observations [1,2]. These discrepancies are often addressed by a selection of appropriate values of computational model parameters, e.g., constraint factors or flow stress. The empirical nature of some of these parameters leaves wide room for discussions regarding their appropriate determination and application, which well done, may lead to an improvement of fatigue life forecasting for considered geometries or loading conditions. These empirical fitting parameters, can also explain a large scatter, or the variability as mentioned above, in the theoretical fatigue life predictions conducted by different practitioners even when using the same software program or assessment methodology. [1,2].

The crack tip opening loads can also be measured experimentally using a wide range of techniques - laser interferometry, optical and scanning electron microscopy, electrical potential drop, compliance, digital image correlation and X-ray based methods to name a few [23–41]. Among these techniques, the one, which is based on specimen/structure compliance changes associated with crack closure process is the simplest and most widely utilised. The compliance-based technique has been standardised by the ASTM [30,31]. Using this technique, crack opening loads, P_{op}, or opening stress intensity factors, K_{op}, or opening load ratios, U, have been obtained for various materials, geometries, and load ratios(R-ratios) over the past fifty years. However, most of these results have been obtained under constant amplitude loading (CAL) conditions or specific loading scenarios, e.g. after a single overload cycle or for block loading sequences.

Despite a wide range of available experimental techniques, none of these techniques is applicable or practical for the evaluation of crack opening loads for large numbers of consecutive cycles, which are representative of real-world applications. The latter usually involve hundreds of thousands or even millions of fatigue cycles of variable amplitude and are typically related to the high-cycle fatigue regime.

Moreno with colleagues [4] were, perhaps, the first, to present experimental measurements of crack tip opening load values using a modified compliance method for consecutive load cycles (total of 20 cycles). The applied load sequence of variable amplitude is characterised by a relatively high R-ratios, see Fig. 1, and absence of significant overloads and underloads. The experiments were conducted on a compact tension (CT) type specimen with 50-mm width and 12-mm (1/2 in.) thickness manufactured from an Al 2024-T351 plate that was cut off in the TL direction. The yield stress and the ultimate tensile strength of the Al 2024-T351 plate were 325 and 470 MPa, respectively. Other basic mechanical properties can be found in [4].

The obtained experimental results from [4] were very surprising and demonstrated that the crack tip opening loads change abruptly from cycle to cycle. This experimental observation is in a contradiction to several life assessment methodologies, which rely on the crack tip opening loads averaged over a large block of the fatigue cycles. To verify this counterintuitive behaviour of P_{op} the researchers also conducted numerical simulations of the crack behaviour under the same load sequence using NASGRO software, which was adapted for cycle-by-cycle

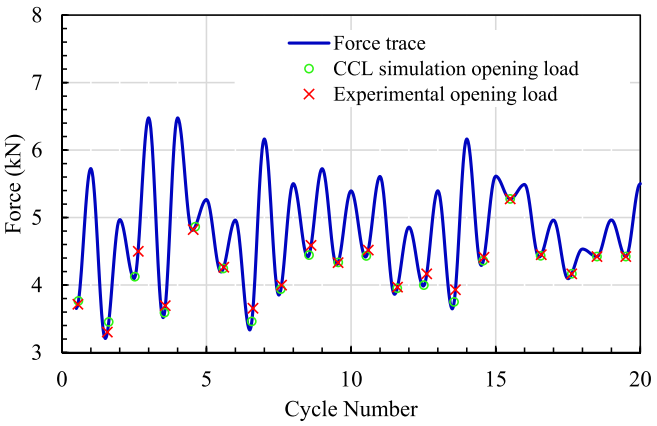

Fig. 1. The loading sequence, experimental and numerical results of crack-tip opening loads for CT specimen manufactured from 2024-T351 aluminium alloy, Moreno et al. (2019) [4].

analysis of crack tip opening loads [42]. Despite some differences in the values of P_{op}, see Fig. 1, the numerical calculations were largely consistent with the experimental data and displayed the same behaviour (i.e., abrupt change in the crack opening values from cycle to cycle). Such a behaviour, in particular, indicates that the crack opening and closure processes might not significantly affected by the past loading history and have relatively "short" memory for the considered load sequences dominated by high R-ratio content and relatively thick specimens.

A step advance, made in 2023 by the authors of this article, is the development and validation of a new experimental procedure for cycle-by-cycle evaluation of crack tip opening loads for realistic loading sequences containing millions of fatigue cycles [40,41]. The procedure utilised an advanced piezoelectric strain gauge, which is several orders of magnitude more sensitive than conventional resistive strain or clip gauges, providing a new way to measure nonlinearities produced by the crack closure process [43]. The procedure made possible to investigate cycle-by-cycle crack tip opening loads for various load spectra, such as the one shown in Fig. 2. This particular test duration was 1.2 million cycles of variable amplitude and comprised of approximately three consecutive applications of a military transport aircraft load spectrum to CT specimens manufactured from Al 7075-T7351 plate, which is a common aerospace grade. The yield stress and the ultimate tensile strength of the Al 7075-T7351 plate was 450 and 520 MPa, respectively. The histograms showing the distributions of applied loads and load ratios for the military transport aircraft spectrum are displayed in Fig. 3.

The outcomes of the experimental evaluation of the crack tip opening loads for the applied load sequence as described above are presented in Fig. 4, in terms of the commonly accepted (for CAL) parameters, i.e., the load ratio, R, and the opening load ratio, U, [3–7] defined as

$$R = \frac{P_{min}}{P_{max}} \tag{1a}$$

and

$$U = \frac{P_{max} - P_{op}}{P_{max} - P_{min}} \tag{1b}$$

For VAL, the maximum load values, P_{max}, can be related to loading, $P^{(n)}_{max}$, or unloading $P^{(n-1)}_{max}$, parts of the fatigue cycle, see Fig. 2 for illustration. The experimental results in Fig. 4a corresponds to the case when $P^{(n)}_{max}$ and $P^{(n)}_{min}$ as well as the crack tip opening value, $P^{(n)}_{op}$, correspond to the loading part of fatigue cycle. The deficiency of this definition, which has been used in some previous studies, is obvious as, e.g., the maximum load, $P^{(n)}_{max}$, does not relate to (or influence) $P^{(n)}_{op}$. This is because $P^{(n)}_{max}$ related to loading part of the cycle is applied after the

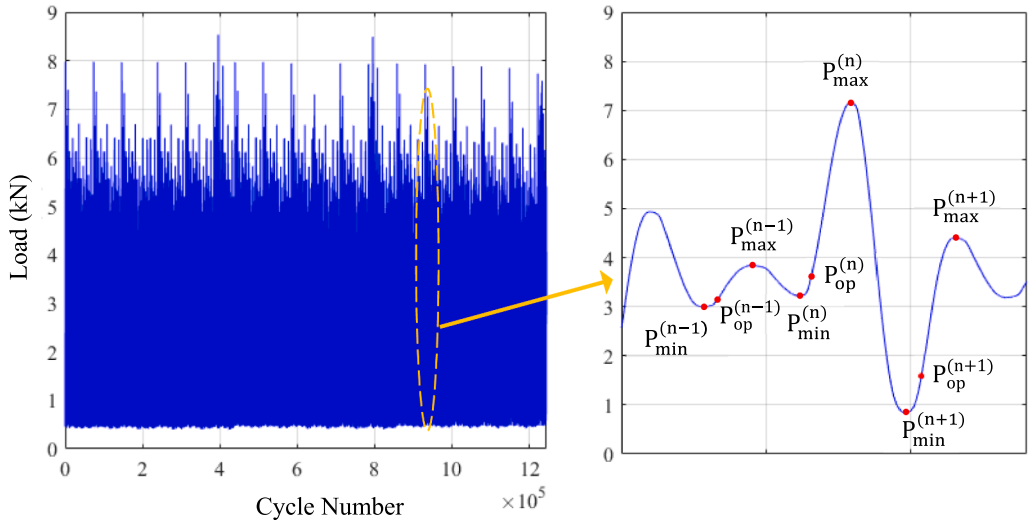

Fig. 2. Military transport aircraft load spectrum [41] (left figure) with the histograms of distributions of applied loads and load ratios shown in Fig. 3 and load definitions in the case of VAL (right figure).

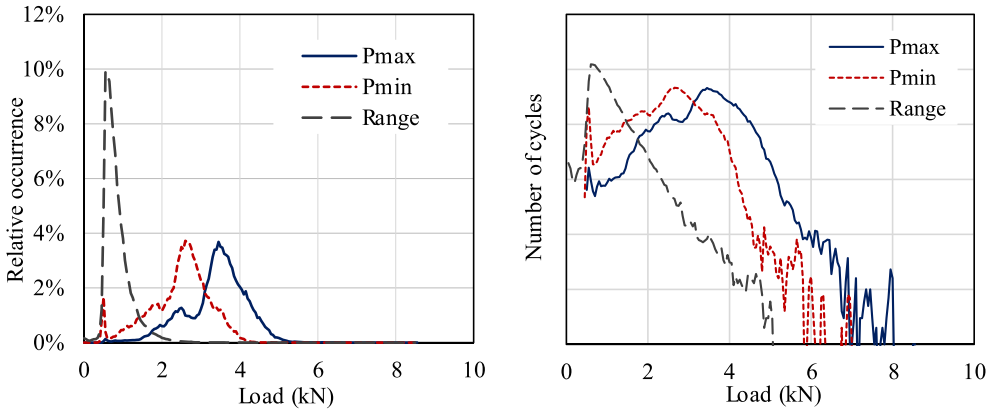

Fig. 3. Histograms showing the distributions of applied loads and load ratios for the military transport aircraft spectrum.

applied load has reached $P_{op}^{(n)}$. Therefore, the experimental and theoretical results presented in terms of common parameters R and U in the case of VAL have to be treated with caution.

Fig. 4b shows the similar results when P_{max} in Eq. (1) is related to the unloading part of the fatigue cycle, see Fig. 2. In contrast to constant amplitude loading (CAL), both representation attempts demonstrate a large scatter and absence of any significant trends. This implies, that common parameters (R, U) utilised to present outcomes of crack tip opening loads under CAL may be inapplicable to the case of VAL. Therefore, one of the objectives of this work is to identify suitable parameters, which could be meaningful in describing experimental measurements of the P_{op} values or opening stress intensity factor, K_{op}.

The present study aims to establish the quantitative relationship between P_{op} and the past loading history, namely the proceeding values of maximum and minimum load values. We postulate that for the considered type of load sequences (high R-ratio content and with no significant overloads and underloads), P_{op} can be well described by a linear function of only two variables: the preceding minimum, $P_{min}^{(n)}$ and maximum loads $P_{max}^{(n-1)}$, see Fig. 2 for notations, or $P_{op}^{(n)} = \alpha \cdot P_{min}^{(n)} + \beta \cdot P_{max}^{(n-1)}$. The coefficients in this equation can be evaluated from direct crack closure measurements or from the analysis of the crack growth data, which can be correlated against $\Delta P_{eff} = P_{max} - P_{op}$ or $\Delta K_{eff} = K_{max} - K_{op}$. ΔP_{eff} and ΔK_{eff} are the effective loading and stress intensity factor ranges, respectively.

The outcomes of this study can be important for the development of effective fatigue life assessment procedures for many practical applications experiencing VAL with relatively high R-ratios. A typical situation associated with such type of loading occurs when the structure is subjected to a constant (dead) load together with variable amplitude loading of a smaller amplitude. One important example of this kind of loading conditions mentioned above is the military (or civil) transport (or passenger) aircraft load spectra.

2. Summary of the Compliance-Based evaluations of crack opening

For the sake of completeness of this paper, a brief introduction to compliance-based measurements of crack tip opening values, P_{op}, is provided in this Section. It should be noted that crack opening is not an event but rather a 3D process, which starts in the middle of the specimen or plate and spreads to free surfaces [3]. Therefore, the experimental evaluation of the crack opening load values depends on the selection of an appropriate threshold or criterion, which would indicate that the tip of the crack is fully open. The experimental measurements can also be affected by crack tip plasticity and other non-linearities as discussed in previous studies [24–32].

The load–displacement (P –δ) curve as originally suggested by Elber

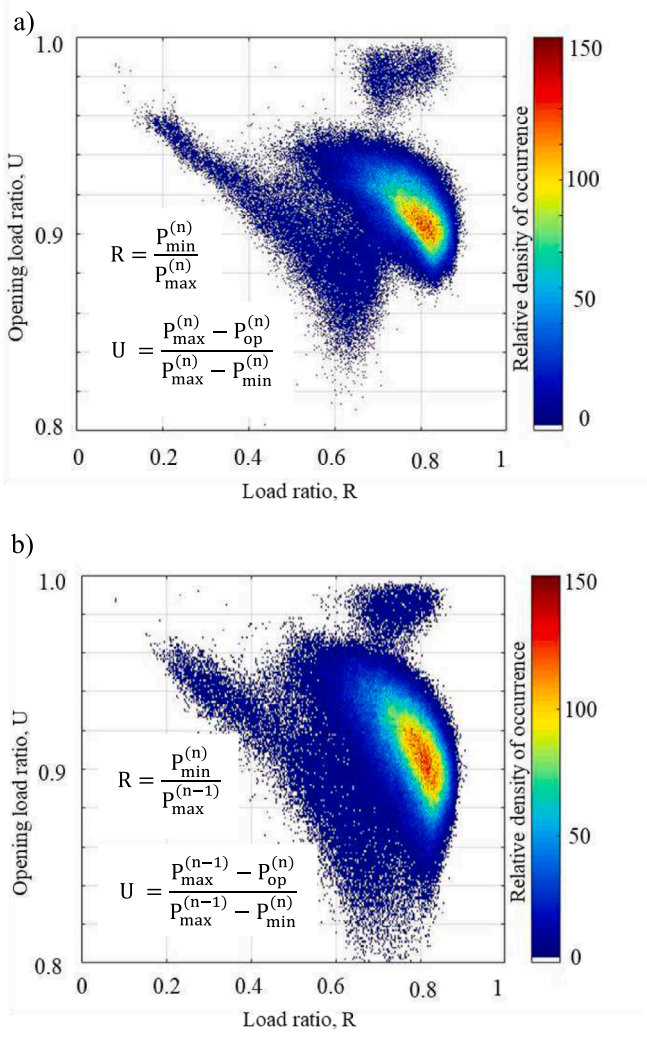

Fig. 4. The opening load ratio versus the load ratio, for the military transport aircraft spectrum shown in Figs. 2 and 3. a) R and U evaluated using the current cycle b) R and U evaluated using the maximum load P_{max} in the previous (n-1) cycle.

[30] or the load-differential displacement ($P - \Delta\delta$) curve, see Fig. 5, as proposed by Kikukawa [33], are typically used in the compliance-based evaluation methods to determine crack tip opening load values. The nonlinear parts of these curves at low load values are attributed to the effect of crack closure on the overall specimen compliance response. The evaluation of the load corresponding to the moment when the crack is fully opened (no contact between crack surfaces) involves the analysis of both the loading and unloading portions of a load cycle. Normally, the load–displacement curve is discretised and a straight line is fitted to the upper portion of the unloading part of the load cycle. From this, the compliance value is determined. This value corresponds to the situation when the crack is fully opened. On the loading portion of the load cycle, straight lines are fitted using the least-squares method producing overlapping segments of the load–displacement curve. The length of these segments (as a percentage of the overall load range) is called the span, and the overlap of segments is determined by a parameter called 'shift'. An appropriate selection of the optimum span-shift combination, which would provide consistent values, is not a simple task and can be quite challenging, specifically in the case of VAL. A general guidance to the selection of the span-shift combination values is provided by the ASTM standards [30,31]. The effect of these values on the measurement of crack tip opening loads was also a subject of a number of research articles in the past.

The determination of the crack tip opening load or opening stress intensity factor values (P_{op} or K_{op}) also requires a threshold value as discussed above. ASTM standard [31] suggests using 2 % compliance offset as a threshold, however, the standard also allows to use other threshold values, as well as other measures, such as the standard deviation of the open crack compliance offset.

The specimen/structure compliance can be measured using various strain sensors; the most common are resistive back-face strain gauge and clip gauge (extensometer) as shown in Fig. 6. Recently, the authors of this article proposed to use a piezoelectric strain gauge, which is manufactured by PCB Piezotronics. The claimed broadband resolution of this strain gauge is 0.6 nε [43] – several orders of magnitude higher than traditional resistive strain gauges, which makes it particular suitable for the detecting of very small non-linearities associated with the crack closure/opening process. The details of this procedure, a comparison between different strain gauges, effects of the shift parameter and the threshold values on P_{op} measurements were reported previously in [40,41].

Fig. 7 shows typical compliance measurements using all there gauges for the same fatigue cycle. It is clear that the piezoelectric strain gauge provides significantly more consistent results compared to the resistive strain and clip gauges. Thus, a piezoelectric strain gauge is highly suitable for real-time cycle-by-cycle measurements of crack closure, permitting a large number of fatigue cycles of variable amplitude to be analysed.

3. Analysis of experimental and numerical data

3.1. Analysis of experimental results for short loading sequences

The suitability of the proposed linear function for the opening load, $P_{op}^{(n)} = \alpha \cdot P_{min}^{(n)} + \beta \cdot P_{max}^{(n-1)}$ is first examined for the experimental data obtained by Moreno et al. [4], some of which is displayed in Fig. 1. As mentioned previously, the experiments were conducted on a compact tension (CT) type specimen with 50-mm width and 12-mm thickness made of 2024-T351 aluminium alloy that was cut off in the TL direction.

The specimen was pre-cracked under constant amplitude loading up to a crack length of 15 mm. Thereafter, a random load spectrum (hereon named "Random Spectrum 1"), containing 25,000 cycles, was repeated until a final crack length of 26 mm was reached after 703,840 cycles. The statistical properties of this random spectrum are provided in Table 1. The opening loads were calculated from the back-face strain gauge measurements and using the modified compliance method for 20-cycle blocks at crack lengths of 24 mm, 25 mm, and 26 mm (the last of these is shown in Fig. 1). An identical specimen was subjected to a different random spectrum (named "Random Spectrum 2"), with statistical properties summarised in Table 2. For the specimen subjected to the second random spectrum, the final crack length of 26 mm was reached after 1,189,200 cycles. Both spectra are characterised by high mean stress (or high R-ratio content) and relatively few small overloads and underloads. The loading sequence and experimentally determined opening load values for 20-cycle sequences are shown for both random spectra in Fig. 8.

A simple least-squares fit is used to estimate the coefficients of the function - $P_{op}^{(n)} = \alpha \cdot P_{min}^{(n)} + \beta \cdot P_{max}^{(n-1)}$, these coefficients are summarised in Table 3 for the different crack lengths and spectra. As shown in Fig. 9, the linear fit correlates very well with the experimental measurements and the predictions are within ± 5 % for all cycles. The preliminary analysis conducted in this Section suggests that the simple method is promising for the spectra under consideration. Further investigations, including effects of experimental uncertainty, memory effects, and low R-ratios, are conducted in the remainder of this paper.

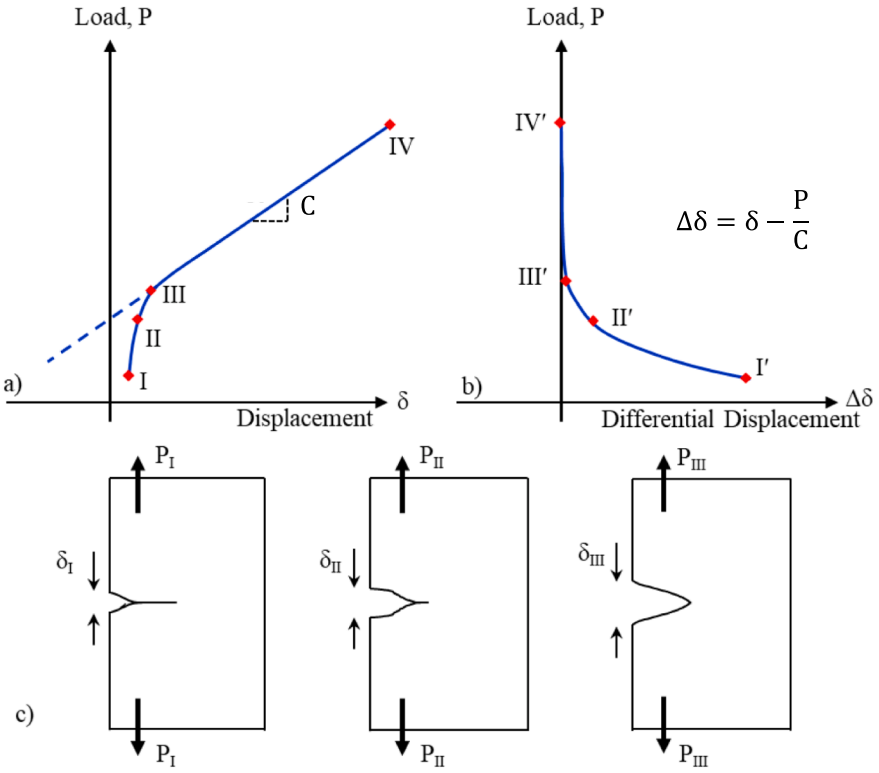

Fig. 5. Crack opening measurements using a) conventional ASTM method, and b) unloading elastic compliance method according to [28] during the crack opening process c).

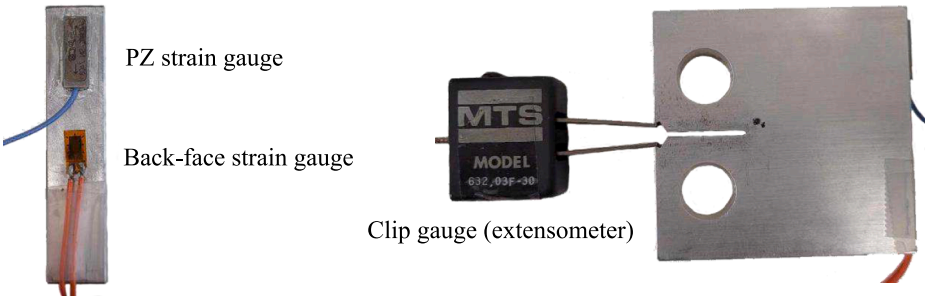

Fig. 6. CT specimen equipped with the piezoelectric strain sensor, resistive strain and clip gauges. Specific dimensions of the specimens manufactured from 7075-T7351 aluminium alloy, which were utilised to produce data presented in Fig. 4, can be found in Refs [40,41].

3.2. Analysis of numerical results for short sequences

The proposed linear function for the opening load can also be applied to the numerically predicted crack tip opening load. For the 20-cycle sequence shown in Fig. 1, Moreno et al. [4] also estimated the opening load using a calibrated strip-yield model in the NASGRO software using the constant and variable constraint-loss options, CCL and VCL, respectively [42]. In both experimental results and numerical simulations, the crack tip opening load was found to fluctuate from cycle to cycle, rather than changing smoothly over a period of several cycles. The fit coefficients obtained using the numerical results are listed in Table 4, and are essentially the same as the coefficients obtained for the experimental results for the same load sequence (Table 3). Moreover, the fit correlates very well with the NASGRO simulations, with a much lower root mean squared error compared to the opening load results obtained from back-face strain gauge data. The reduced fit error is presumably due to lower uncertainty in the numerical calculation of opening loads, compared to experimental measurements, which can be influenced by the poor signal to noise ratio of resistive strain gauges. The fit results, shown in Fig. 10 suggest that the use of advanced fatigue crack growth software (such as NASGRO or FASTRAN) may not be necessary at all for certain types of variable amplitude spectra, such as those under consideration in the present work.

3.3. Investigation of memory effects using higher-order regression models

The small sample size of 20 cycles as considered above limits the analysis of higher order autoregressive models. In this section, we analyse higher order autoregressive models with the data set recently published in [41] representative of a military transport aircraft spectrum. A larger data set now permits the assessment of memory effects. This section presents high-order regression modelling results for the 1.2 million loading cycles or approximately three consecutively applied military transport aircraft spectra as shown in Fig. 2. For the latter dataset, the P_{op} values were measured in real-time for the entire loading sequence using the piezoelectric strain gauge readings. The statistical

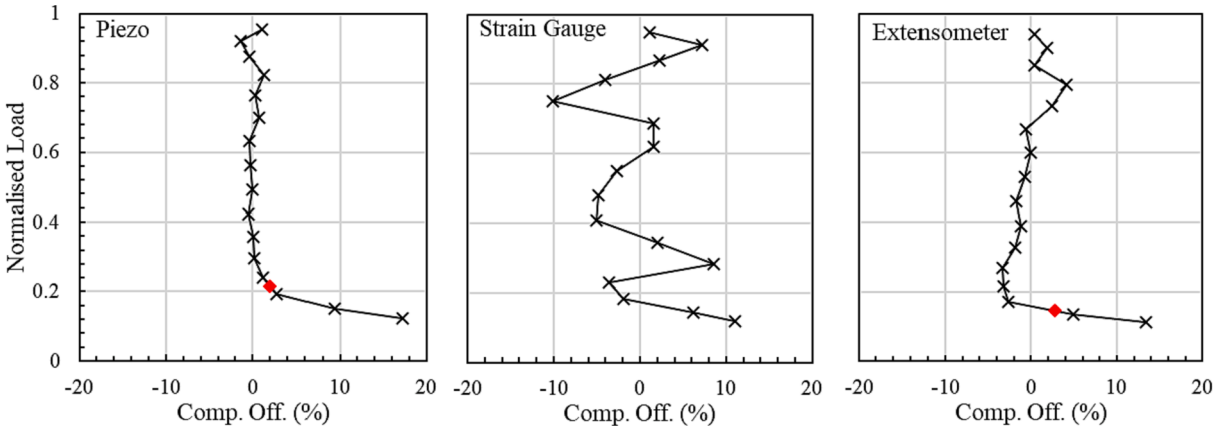

Fig. 7. Compliance curves obtained using the piezoelectric strain sensor, back-face resistive strain gauge, and clip gauge. Rhombus corresponds to the identified crack tip opening load (it is not detected in the case of the use of resistive strain gauge).

Table 1
Statistical properties of Random Spectrum 1.

Peaks (N)					Valleys (N)					Range (N)				
max	min	mean	S.D	RMS	max	min	mean	S.D	RMS	max	min	mean	S.D	RMS
7887	3418	5470	519	5494	6076	2050	4242	517	4274	4717	0	1227	732	1429

Table 2
Statistical properties of Random Spectrum 2.

Peaks (N)					Valleys (N)					Range (N)				
max	min	mean	S.D	RMS	max	min	mean	S.D	RMS	max	min	mean	S.D	RMS
7585	3449	5365	557	5394	6386	2050	4343	558	4379	3832	0	1023	552	1162

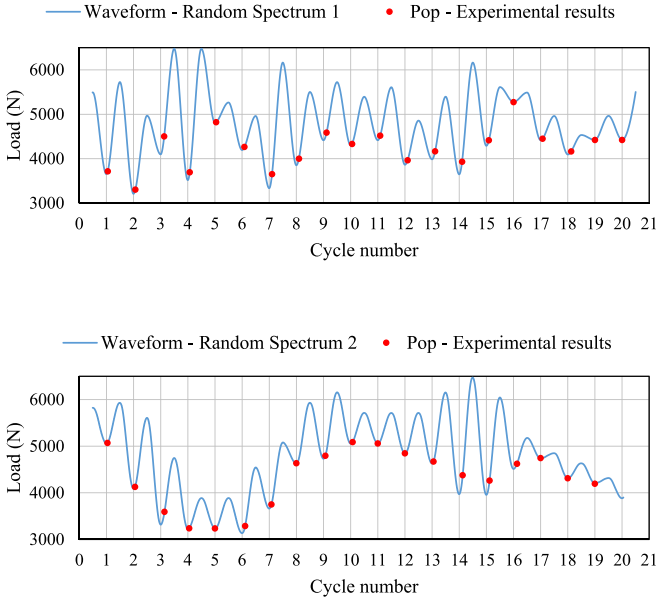

Fig. 8. Experimental results for opening loads for two identical specimens at the same crack length (26 mm) but subjected to different spectra (histories).

properties of this spectrum are provided in Table 5 and histograms shown in Fig. 4.

The methodology for investigating memory effects is based on high-order Autoregressive-Exogenous (ARX) models [44]. The ARX model used herein assumes that the output of the current cycle, $P_{op}^{(n)}$ is independent of past values of P_{op} but depends on the past k values of two exogenous inputs, namely $P_{min}^{(n-j)}$, and $P_{max}^{(n-j-1)}$, $j = 0, \cdots, k-1$. The ARX model of order k is defined as:

$$P_{op}^{(n)} = \alpha_0 P_{min}^{(n)} + \alpha_1 P_{min}^{(n-1)} + \cdots + \alpha_k P_{min}^{(n-k-1)} + \beta_0 P_{max}^{(n-1)} + \beta_1 P_{max}^{(n-2)} + \cdots + \beta_k P_{max}^{(n-k-2)}, \quad (2)$$

where α_j and β_j are unknown weights. Defining the backward shift operator as $\zeta^{-j} x_i^{(n)} = x_i^{(n-j)}$, the regression equation can be written compactly as

$$P_{op}^{(n)} = \sum_0^{k-1} \alpha_j \zeta^{-j} P_{min}^{(n)} + \sum_0^{k-1} \beta_j \zeta^{-j} P_{max}^{(n-1)}. \quad (3)$$

For $k = 1$, Eq. (3)reduces to the simple linear function examined in previous sections. The significance of the memory effect is investigated by varying the regression order k and evaluating the changes in the fit error. If the memory effect is not significant for a given spectrum, increasing the regression order (i.e., the number of past cycles to include in the fitting function) will not result in a significant reduction in the fit error. The sensitivity study conducted in Fig. 11 demonstrates that while increasing the regression order (or longer memory effects) improves the

Table 3
Fit coefficients for the function $P_{op}^{(n)} = \alpha \bullet P_{min}^{(n)} + \beta \bullet P_{max}^{(n-1)}$. for Moreno et al (2019) experimental data.

Dataset	α	β
Random Spectrum 1, $a = 24$ mm	0.92	0.08
Random Spectrum 1, $a = 25$ mm	0.85	0.14
Random Spectrum 1, $a = 26$ mm	0.95	0.05
Random Spectrum 2, $a = 26$ mm	0.84	0.14
Average	0.90	0.10

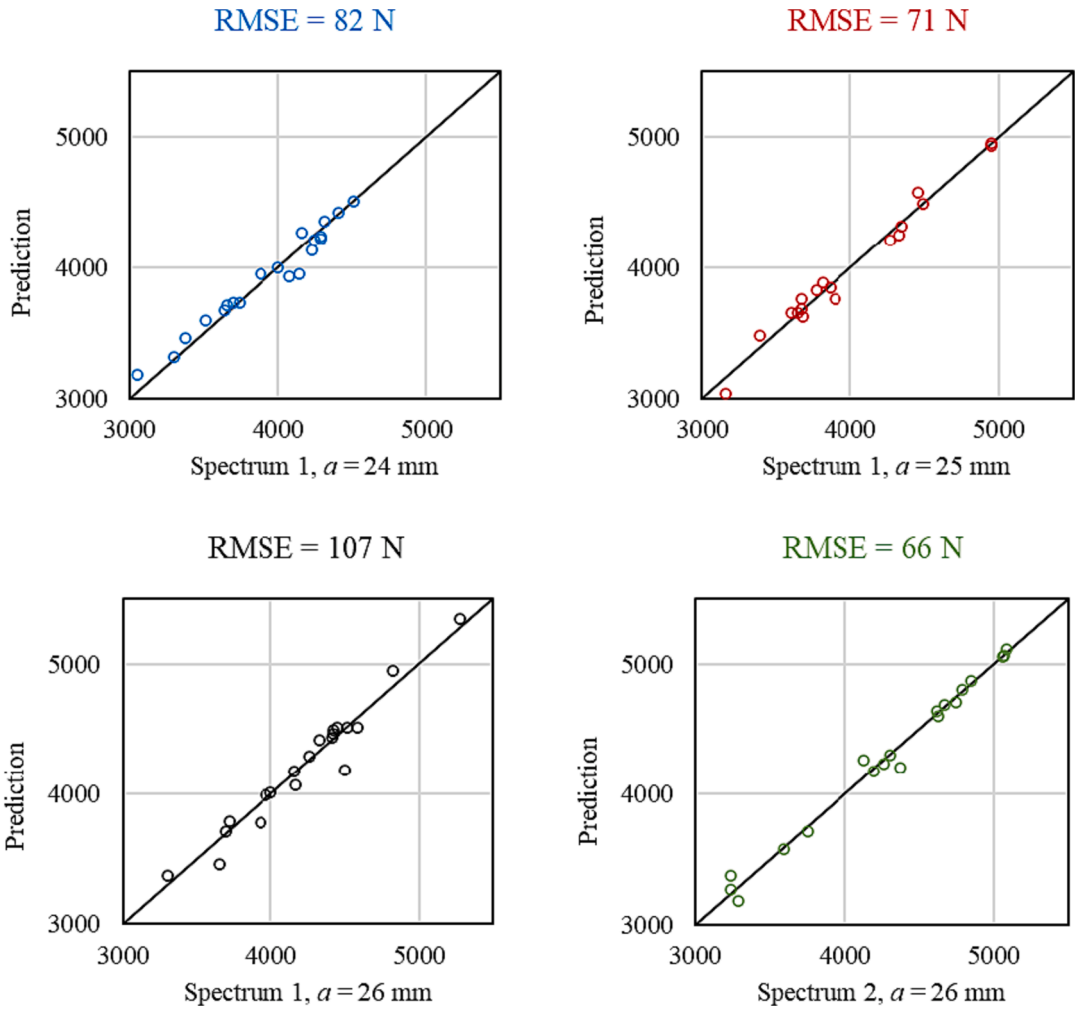

Fig. 9. Comparison of the experimentally determined values of the opening loads against the linear fit predictions obtained using the coefficients listed in Table 3 (all loads expressed in Newtons). RMSE stands for the root-mean-square error.

Table 4
Fit coefficients for the function $P_{op}^{(n)} = \alpha \bullet P_{min}^{(n)} + \beta \bullet P_{max}^{(n-1)}$ for numerical data obtained by Moreno et al (2019) for Random Spectrum 1 at $a =$ 26 mm.

Numerical Method	α	β
Constant-Constraint Loss (CCL) Option	0.935	0.059
Variable-Constraint Loss (VCL) Option	0.938	0.057

fit, these improvements are negligible. Increasing the regression order (number of past cycles included in fit) from 1 to 100 only results in a 2 % reduction in the root mean squared error. Hence, the higher order autoregressive model does not offer significant improvements over the simple two-parameter linear function considered previously for the military transport aircraft spectrum considered in this section. The fitted two-parameter model in this instance is obtained as

$$P_{op}^{(n)} = \alpha P_{min}^{(n)} + \beta P_{max}^{(n-1)} = 0.96 P_{min}^{(n)} + 0.05 P_{max}^{(n-1)}. \quad (4)$$

The coefficients α, β, in Eq. (4) are almost identical to the coefficients in Table 4. This is somewhat expected due to the similarities between the two datasets in terms of material (Aluminium alloys), geometry (50 mm wide and 12 mm thick CT specimens) and loading conditions (high R-ratio spectra with similar statistical properties in Table 1 and Table 5.

3.4. Investigation of crack tip opening loads at low R-ratios using a nonlinear regression model

For CAL, where the maximum and minimum loads are the same for all cycles, Eq. (4) suggests the following relationship between the opening load ratio, U, and the loading ratio,R,

$$U = \frac{1 - \beta - \alpha R}{1 - R}, \quad (5)$$

where the parameters U and R are defined in Eq.(1). For constant values of the parameters α and β, Eq. (5) predicts a relatively weak dependence of U on R. At $R = 0$, when crack closure is expected to be significant, Eq. (5)predicts $U = 1 - \beta \approx 1$ for the fitting coefficients obtained in the previous sections (high R-ratio datasets). In order to extend the usefulness of the proposed approach to lower R-ratios ($R < 0.5$), the coefficients α and β must not be constant, but instead functions of $P_{min}^{(n)}$ and $P_{max}^{(n-1)}$, i.e., $\alpha = \alpha\left(P_{min}^{(n)}, P_{max}^{(n-1)}\right)$, $\beta = \beta\left(P_{min}^{(n)}, P_{max}^{(n-1)}\right)$ and the function becomes:

$$P_{op}^{(n)} = \alpha\left(P_{min}^{(n)}, P_{max}^{(n-1)}\right) \cdot P_{min}^{(n)} + \beta\left(P_{min}^{(n)}, P_{max}^{(n-1)}\right) \cdot P_{max}^{(n-1)} \quad (6)$$

To this end, a nonlinear regression model, namely a decision tree ensemble model, is developed using the bootstrap aggregation method. The nonlinear dependence of α and β on $P_{min}^{(n)}$ and $P_{max}^{(n-1)}$ is not obtained in closed-form (it is not an analytical function), instead it is in the form of a

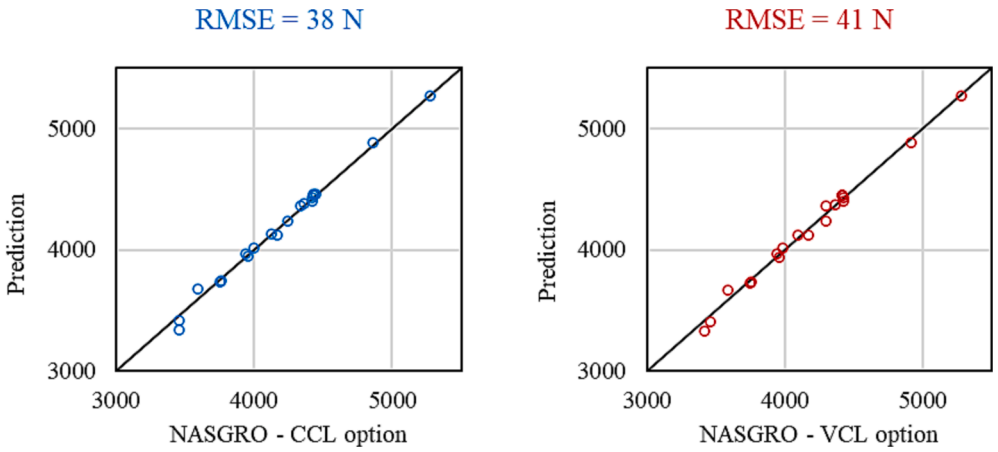

Fig. 10. Comparison of the numerical values of the opening loads obtained from experimentally calibrated NASGRO models against the linear fit predictions obtained using the coefficients listed in Table 3 (all loads expressed in Newtons).

Table 5
Statistical properties of the military transport aircraft spectrum.

Peaks (N)					Valleys (N)					Range (N)				
max	min	mean	S.D	RMS	max	min	mean	S.D	RMS	max	min	mean	S.D	RMS
8535	451	3359	784	3449	6975	396	2487	766	2602	5108	0	872	352	940

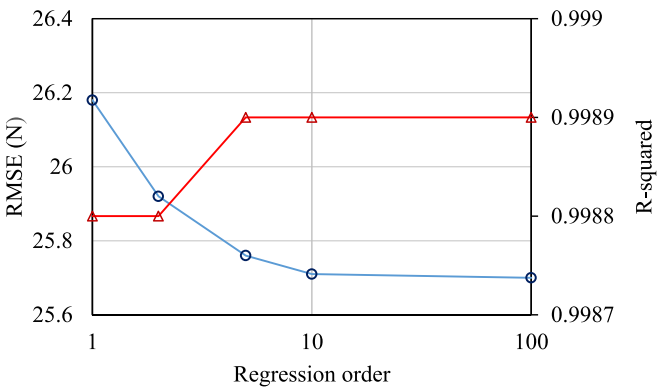

Fig. 11. Effect of regression order on the fit error for the military transport aircraft spectrum.

black-box model trained using the aircraft spectrum [40,41].

The decision tree ensemble model is a popular machine learning algorithm, suitable for datasets where data can be analysed non-sequentially [45]. The sensitivity analysis conducted in the previous section suggests that values of the two regressors, namely the minimum load of the current cycle, $P_{min}^{(n)}$, and the maximum load of the previous cycle, $P_{max}^{(n-1)}$ are sufficient for spectra with insignificant memory effect, i.e., the dataset $\left\{P_{op}^{(n)}, P_{min}^{(n)}, P_{max}^{(n-1)}\right\}$ can be analysed in any arbitrary order of the cycle number n. In line with best practice for regression analysis, the data is centred and scaled to have zero mean and unit standard deviation prior to fitting. The entire spectrum of 1.2 million cycles is split into 80 % data for training the nonlinear regression model, and 20 % data for evaluating the model. The relative prediction errors of the linear regression model given by Eq. (4) and the nonlinear regression model given by Eq. (6) are compared in Fig. 12 for the 240,000 cycles set aside for model testing. Both models provide similar root mean squared error values and similar distribution of relative errors (75 % of predictions within ± 1 % of measured values).

To verify the model predictions, a separate experimental dataset from [35] was used. This data set contains constant amplitude block loading at low R-ratios as well. The experimental results are obtained from [34,35] where block loading was applied to an identical specimen as the one subjected to military transport aircraft spectrum, with P_{max} = 4 kN and P_{min} between 0.08 kN and 2 kN ($0 < R \leq 0.5$). Fig. 13 shows the performance of the linear regression (LR) and nonlinear regression (NLR) models against the experimental results for crack length a = 26.6 mm (a/W = 0.52). Both models provide excellent correlation with the experimental data for intermediate values of stress ratio, i.e., R = 0.5. At low stress ratios, particularly $R < 0.2$, the nonlinear regression model provides a significantly better fit against the experimental data.

It must be highlighted that only around 0.2 % of the training dataset, as shown in the histogram in Fig. 3 contains cycles between $0.08 < R < 0.2$. However, given the large dataset this still equates to 1920 cycles. Despite the limited data, the nonlinear regression model successfully captures the dependence of opening load on R-ratio. With additional training data at zero and low mean stress, it is expected that the accuracy of the nonlinear regression model can be improved further. Hence, the methodology presented in this paper, namely data-driven crack tip opening load approach, is a promising alternative to past theoretical and numerical predictive models.

3.5. Selection of parameters to represent experimental data for VAL

Based on the data obtained from the military transport spectrum and the short random spectra analysed, the outcomes of this work suggest that $R_{eff} = P_{op}^{(n)}/P_{max}^{(n-1)}$ is a linear function of $R = P_{min}^{(n)}/P_{max}^{(n-1)}$ or

$$R_{eff} = \frac{P_{op}^{(n)}}{P_{max}^{(n-1)}} = \alpha \frac{P_{min}^{(n)}}{P_{max}^{(n-1)}} + \beta = \alpha \cdot R + \beta \tag{7}$$

Therefore, parameters R_{eff} and R as defined above can be appropriate to present experimental results related to crack tip opening loads for the type of fatigue loading considered in this work (i.e. relatively high R-ratio content and absence of significant overloads and underloads).

Indeed, Figs. 14 and 15 present experimental and numerical results for Random Spectra 1 and 2 and military transport aircraft load spectrum as described above. All experimental results confirm the linear relationship between crack tip opening load and two preceding turning

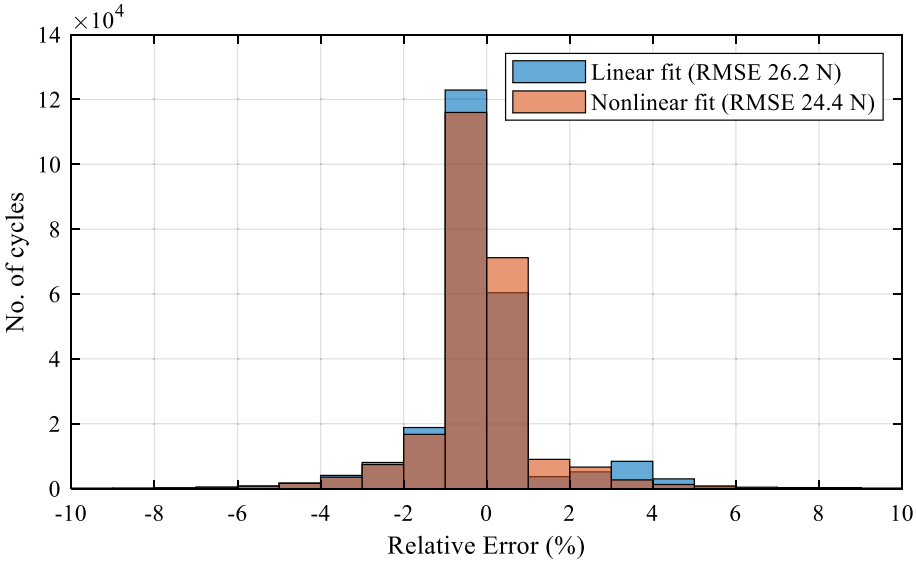

Fig. 12. Relative error distribution of the opening load predictions obtained using the linear regression model (blue) and nonlinear regression model (red). (For interpretation of the references to colour in this figure legend, the reader is referred to the web version of this article.)

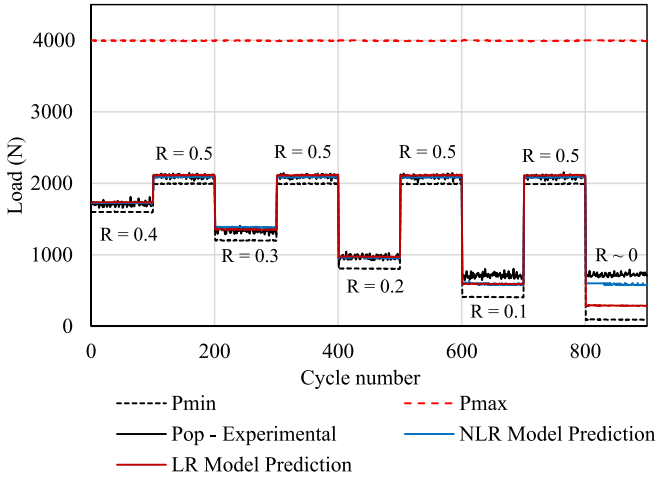

Fig. 13. Comparison of the linear (solid red) and nonlinear (blue) regression models to experimentally derived opening load values (solid black) for low R-ratios. Some variations of the experimental values (solid black lines) within blocks can be noted, which confirm the consistency of the cycle-by-cycle P_{op} measurements using the piezoelectric gauge. (For interpretation of the references to colour in this figure legend, the reader is referred to the web version of this article.)

points. This would suggest that there exists a (practical) class of fatigue crack growth scenarios that could well be described by this linear relationship. The influence of crack shape and specimen geometry has not yet been explored, nor the conditions that would begin to invalidate this observation and remain the focus of future investigation.

While the results presented in the work are appealing due to their simplicity, it should be noted that these observations may not extend to other materials. This could be due to other more dominant closure effects such as roughness induced closure. The geometry of the specimens as well as the crack geometry itself will also impact plasticity-induced crack closure process and, as mentioned above, will be the focus of future research. Although the spectra considered in this work displayed strong linearity it is possible that the same spectra given a different crack growth scenario could experience greater levels of closure. Again this is an area for further exploration.

4. Discussion and conclusion

In this article, we suggested a new data-driven approach to evaluate crack tip opening loads for large number of cycles of variable amplitude. In particular, we verified that crack tip opening loads, P_{op}, for load spectra with relatively high R-ratio content and without significant underloads and overloads, can be adequately predicted by a linear function of the preceding minimum and maximum values of the applied loading sequence with no loading memory effects beyond these two closest turning points. The low R ratio content that does display a more significant influence on the opening load only represented 0.2 % of the data. The discrepancies between the derived equation and experimental as well as numerical results are minor, and are expected have no effect on the fatigue life evaluations, which utilise the crack closure concept. We also verified that the utilisation of machine learning algorithms can further extend the applicability range of the proposed approach, specifically for fatigue cycles with low R-ratio. Despite the complexity of the spectrum analysed, non-linear behaviours observed for low R-ratio spectrum content were adequately captured.

The main practical outcome of this work is that for the considered type of loading sequences (or load spectra) and relatively thick specimens or plate structures there is no need in extensive, sometime time-consuming, and often unreliable, theoretical analysis and numerical simulations. The crack tip opening model, which is essentially the two-parameter linear equation, can be constructed from direct measurements of crack opening loads or even numerical simulations for a limited number of fatigue cycles. It is also possible to obtain this equation from the crack growth data under variable amplitude loading using the best fit approach. The obtained dependencies for P_{op}, which is directly related to K_{op}, can be further utilised for fatigue life assessments using the so called master curve, which links $\Delta K_{eff} = K_{max} - K_{op}$ to crack growth rates.

The use of the P_{op} and K_{op} values in fatigue life calculations also requires a cycle counting algorithm, which is elementary in the case of constant amplitude loading. In our previous work [41] Fig. 11, it was found that the linear peak-valley (LPV) cycle counting algorithm provides the most accurate evaluation of fatigue life of CT specimens subjected to military transport aircraft spectrum shown in Fig. 2. At the same time, it is easy to demonstrate that LPV algorithm is inapplicable to certain types of fatigue loading, e.g., “Christmas tree” type loading. Therefore, the development of a universal cycle counting algorithm, which would be valid for different types of loading spectra, represents

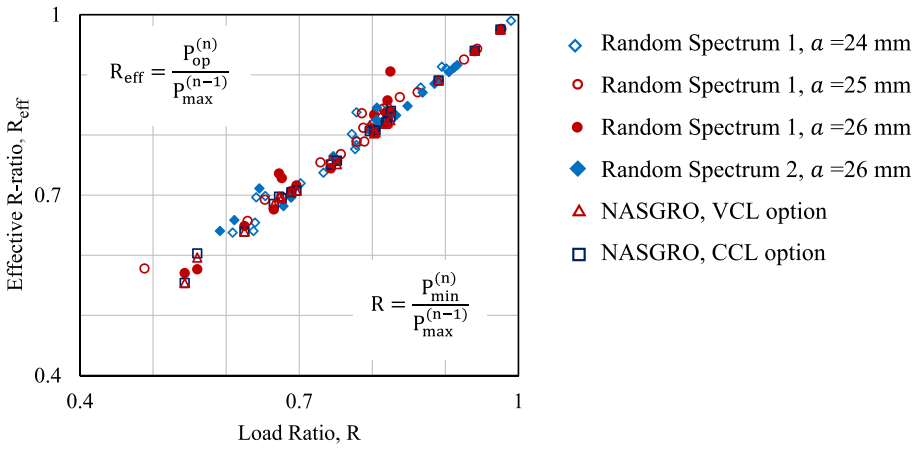

Fig.14. Outcomes of crack tip opening loads for Random Spectra 1 and 2 in terms of R_{eff} and R defined using unloading part of fatigue cycle.

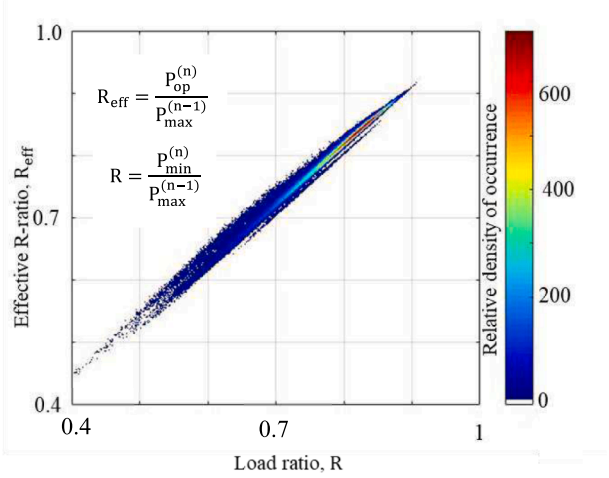

Fig.15. Outcomes of measurements of crack tip opening loads in 7075-T7351 CT specimen for military transport aircraft load spectrum (around 1.2 million measurement points).

another significant challenge in fatigue. The new procedure [40,41] for cycle-by-cycle crack tip opening measurements synchronised with the crack growth data can serve as a foundation for the investigation and development of such universal algorithm(s) in the future. Indeed, prospective cycle counting algorithms can only be tested and evaluated if crack growth data and cycle-by-cycle values for P_{op} (or K_{op}) are both available for sufficiently large sets of consecutive fatigue cycles.

Obviously, the most intriguing question is - if the same data-driven approach can be applied to more "aggressive" or "chaotic" fatigue loading sequences, which can also contain large overloads and underloads or to thin specimens where the plasticity effects are more pronounced. It is believed that this new approach can be generalised for such sequences and cases by utilising the latest advances in experimental techniques (the evaluation of crack tip opening loads for large numbers of cycles) and machine learning algorithms, which can help to establish hidden dependencies between P_{op} or K_{op} and the past (short and long) loading history by analysing large data sets. One simple example has been provided in this article and shown to capture non-linear closure behaviour for block loading.

CRediT authorship contribution statement

Andrei Kotousov: Conceptualization, Methodology, Writing – original draft. **James Hughes:** Methodology, Data curation, Investigation, Formal analysis, Writing – review & editing. **Aditya Khanna:** Methodology, Formal analysis, Investigation, Validation, Writing – review & editing. **Belen Moreno:** Methodology, Investigation, Validation, Writing – review & editing. **Chris Wallbrink:** Conceptualization, Investigation, Writing – review & editing.

Declaration of competing interest

The authors declare that they have no known competing financial interests or personal relationships that could have appeared to influence the work reported in this paper.

Data availability

Data will be made available on request.

Acknowledgement

This research was supported by the Australian Research Council's Discovery Projects funding scheme (project DP240103201) and the Defence, Science and Technology Group. Further, the authors would like to thank Mr Beau Krieg for his continued and ongoing discussions. Finally, Mr Matthew Gillet for his efforts in facilitating the fatigue tests.

References

[1] Khanna A, Kotousov A. The potential for structural simulation to augment full scale fatigue testing: A review. Prog Aerosp Sci 2020;121:100641.
[2] K. Walker A. Grice JC. Newman Jr 2023. Improved capability to model long cracks in high-strength aerospace alloys. A Review of Australian Aeronautical Fatigue and Structural Integrity Investigations During May 2021 to April 202. ICAF, can be accessed. https://www.icaf.aero/ajax/showPDF.php?filename=ICAF2023_National_Review_Australia.pdf&pad=docs/National_reviews/&year=2023.
[3] Kujawski D. Discussion and comments on Kop and ΔKeff. Materials 2020;13:4959.
[4] Moreno M, Lopez-Crespo P, Cruces A, Dominguez J. Estimation of the opening load under variable amplitude loading. Fatigue Fract Eng Mater Struct 2019;(24):2195–204.
[5] Sehitoglu H. Crack opening and closure in fatigue. Eng Fract Mech 1985;21(2):329–39.
[6] Pippan R, Hohenwarter A. Fatigue crack closure: A review of the physical phenomena. Fatigue Fract Eng Mater Struct 2017;40:471–95.
[7] Machniewicz T. Fatigue crack growth prediction models for metallic materials: Part I: Overview of prediction concepts. Fatigue Fract Eng Mater Struct 2013;36(4):93–307.
[8] Elber W. Fatigue crack closure under cyclic tension. Eng Fract Mech 1970;2(1):37–45.
[9] Antunes FV, Branco R, Prates PA, Borrego LF. Fatigue crack growth modelling based on CTOD for the 7050–T6 alloy. Fatigue Fract Eng Mater Struct 2017;40:1309–20.
[10] Borges MF, Lopez-Crespo P, Antunes FV, Moreno B, Prates P, Camas D, et al. Fatigue crack propagation analysis in 2024–T351 aluminium alloy using nonlinear parameters. Int J Fatigue 2021;153:106478.

[11] de Matos PFP, Nowell D. (2007) On the accurate assessment of crack opening and closing stresses in plasticity-induced crack closure problems. Eng Fract Mech 2007; 74(10):1579–601.
[12] Alizadeh H, Hills DA, de Matos PFP, Nowell D, Pavier MJ, Paynter RJ, et al. A comparison of two and three-dimensional analyses of fatigue crack closure. Int J Fatigue 2007;29:222–3.
[13] Zapatero J, Moreno B, González-Herrera A. Fatigue crack closure determination by means of finite element analysis. Eng Fract Mech 2008;75:41–57.
[14] Gonzalez-Herrera A, Zapatero J. Three-dimensional numerical modelling of plasticity induced fatigue crack closure. Eng Fract Mech 2008;75:4513–28.
[15] Antunes FV, Camas D, Correia L, Branco R. (2015) Finite element meshes for optimal modelling of plasticity induced crack closure. Eng Fract Mech 2015;142: 184–200.
[16] Maia RM, Branco R, Antunes FV, Oliveira MC, Kotousov A. Three-dimensional computational analysis of stress state transition in through-cracked plates. Math Comput Sci 2016;2016(10):343–52.
[17] Camas D, Garcia-Manrique J, Moreno B, Gonzalez-Herrera A. Numerical modelling of three-dimensional fatigue crack closure: Mesh refinement. Int J Fatigue 2018; 113:193–203.
[18] Camas D, Garcia-Manrique J, Antunes FV, Gonzalez-Herrera A. (2020) Three-dimensional fatigue crack closure numerical modelling: Crack growth scheme. Theor Appl Fract Mech 2020;108:102623.
[19] Pommier, et al. Fatigue crack propagation and history effects induced by plasticity. Adv Eng Mater 2009;11(9):717–22.
[20] Dugdale D. Yielding of steel sheets containing slits. J Mech Phys Solids 1960;8(2): 100–4.
[21] Codrington J, Kotousov A. A crack closure model of fatigue crack growth in plates of finite thickness under small-scale yielding conditions. Mech Mater 2009;2009 (41):165–73.
[22] JC. Newman Jr II FASTRAN A fatigue crack growth structural analysis program NASA 1992.
[23] Newman Jr JC, Walker KF. Fatigue-crack growth in two aluminum alloys and crack-closure analyses under constant-amplitude and spectrum loading. Theor Appl Fract Mech 2019;100:307–18.
[24] Van Kuijk JJA, Alderliesten RC, Benedictus R. Measuring crack growth and related opening and closing stresses using continuous potential drop recording. Eng Fract Mech 2021;2021(252):107841.
[25] Gama AL. Morikawa SRK.A piezoelectric technique for evaluation of crack closure. Exp Mech 2009;49:871–6.
[26] Toda H, Sinclair I, Buffière J-Y, Maire E, Connolley T, Joyce M, et al. (2003) Assessment of the fatigue crack closure phenomenon in damage tolerant aluminium alloy by in-situ high-resolution synchrotron X-ray microtomography. Phil Mag 2003;83(21):2429–48.
[27] Tong J, Alshammrei S, Wigger T, Lupton C, Yates JR. Full-field characterization of a fatigue crack: Crack closure revisited. Fatigue Fract Eng Mater Struct 2018;2018 (41):2130–9.
[28] Stoychev S, Kujawski D. Methods for crack opening load and crack tip shielding determination: A review. Fatigue Fract Eng Mater Struct 2003;26(11):1053–67.
[29] Kujawski D, Stoychev S. (2003) Parametric study on the variability of opening load determination. Int J Fatigue 2003;25(9–11):1181–7.
[30] Elber W. The significance of fatigue crack closure. ASTM Spec Tech Publ 1971: 230–42.
[31] Standard test method for measurement of fatigue crack growth rates, in Annual Book of ASTM standards. 2009: 647-508.
[32] Yigeng Xu, Gregson PJ, Sinclair I. Systematic assessment and validation of compliance-based crack closure measurements in fatigue. Mater Sci Eng A 2000; 284(1–2):114–25.
[33] M. Kikukawa M. Jono K. Tanaka Fatigue crack closure behavior at low stress intensity levels. in ICM 2 1976.
[34] Newman Jr JC, Yamada Y, James MA. Back-face strain compliance relation for compact specimens for wide range in crack lengths. Eng Frac Mech 2011;78: 2707–11.
[35] Song JH, Chung YI. A review of crack closure measurement by compliance technique and the normalized-extended ASTM method as a currently most refined, practical and simple one. Procedia Eng 2010;2:777–86.
[36] Newman Jr JC, Brot A, Matias C. Crack growth calculations in 7075–T7351 aluminum alloy under various load spectra using improved crack closure model. Eng Fracture Mechanics 2004;71:2347–63.
[37] Andersson M, Persson C, Melin S. Experimental and numerical investigation of crack closure measurements with electrical potential drop technique. Int J Fatigue 2006;28:1059–68.
[38] Ravi P, Naragani D, Kenesei P, Park J-S, Sangid MD. Direct observations and characterization of crack closure during microstructurally small fatigue crack growth via in-situ high-energy X-ray characterization. Acta Mater 2021;205: 116564.
[39] Yusof F, Lopez-Crespo P, Withers PJ. Effect of overload on crack closure in thick and thin specimens via digital image correlation. Int J Fatigue 2013;56:17–24.
[40] Wallbrink C, Hughes JM, Kotousov A. Application of an advanced piezoelectric strain sensor for crack closure measurement. Int J of Fatigue 2023;167:107286.
[41] Wallbrink C, Hughes JM, Kotousov A. Experimental investigation of crack opening loads in an aircraft load spectrum. Int J of Fatigue 2023;2023(171):107560.
[42] NASGRO 6.0, Reference Manual, Fracture mechanics and fatigue crack growth analysis software (version 6.02, September 2010).
[43] Piezotronics, Model 740B02 ICP piezoelectric strain sentor, titanium hsg: Installation and Operating Manual, 2021.
[44] Box GE, Jenkins GM, Reinsel GC, Ljung GM. Time series analysis: Forecasting and control. John Wiley & Sons; 2015.
[45] Zhou ZH. Ensemble methods: Foundations and algorithms. CRC Press; 2012.